Mechanical Deformation Accelerates Protein Ageing

Jessica Valle-Orero⁺,* Jaime Andrés Rivas-Pardo⁺, Rafael Tapia-Rojo, Ionel Popa, Daniel J. Echelman, Shubhasis Haldar, and Julio M. Fernández*

Abstract: *A hallmark of tissue ageing is the irreversible oxidative modification of its proteins. We show that single proteins, kept unfolded and extended by a mechanical force, undergo accelerated ageing in times scales of minutes to days. A protein forced to be continuously unfolded completely loses its ability to contract by folding, becoming a labile polymer. Ageing rates vary among different proteins, but in all cases they lose their mechanical integrity. Random oxidative modification of cryptic side chains exposed by mechanical unfolding can be slowed by the addition of antioxidants such as ascorbic acid, or accelerated by oxidants. By contrast, proteins kept in the folded state and probed over week-long experiments show greatly reduced rates of ageing. We demonstrate a novel approach whereby protein ageing can be greatly accelerated: the constant unfolding of a protein for hours to days is equivalent to decades of exposure to free radicals under physiological conditions.*

Young tissues readily regain their shape after mechanical deformation. Loss of mechanical integrity is a recognizable feature of ageing tissues.[1] Exposure of tissues, such as skin, to UV light generates free radicals which, over time, irreversibly change the constituent tissue proteins, reducing their elastic recoil.[2] Oxidative protein damage caused by modifications in the side chains is closely related to molecular and cellular ageing.[3] For example, irreversible modifications such as carbonylation and carbamylation of protein side chains are hallmarks of ageing and the loss of protein function.[4] All 20 amino acids are potential substrates of oxidative damage[5] that could trigger misfolding, and eventually protein aggregation.[6]

Despite extensive studies on the physics and chemistry of proteins under force,[7] it is unknown how proteins lose their mechanical integrity (ability to respond to force by unfolding and refolding). Upon application of a mechanical force, folded proteins unfold, exposing buried side chains to solution where they are susceptible to random oxidative modifications. For example, reactants such as glutathione and hydroxide can

react with cryptic cysteine residues to block protein folding.[8] However, in contrast to oxidative ageing which is irreversible, such thiol modifications are fully reversible and are part of healthy cellular homeostasis.

A major difficulty in the study of oxidative protein damage is the extremely long time scales involved and the heterogeneity of this chemistry. Given that most proteins are only transiently unfolded in vivo, the probability of oxidative modification of cryptic side chains is low. Nevertheless, damage accumulates over time, particularly in low-turnover proteins. The advent of ultra-stable magnetic tweezers now permits studies of protein dynamics under force over extended time periods.[9] Here, we use magnetic tweezers to monitor the folding dynamics of single proteins placed under force, over time scales of hours to days, and study how they age. We expose single proteins to the cumulative oxidative modifications of cryptic side chains, and study the effect on elasticity. In doing so, we show that keeping a protein in the unfolded state by applying force is a form of accelerated ageing, where decades worth of oxidative damage are compressed into hours. This ageing causes a loss of elasticity, with aged proteins providing 50 % less contractility than younger proteins.

In our experiments, a tandem modular protein was attached by its N terminus to a glass surface using a Halo-Tag,[10] and to a streptavidin-coated paramagnetic bead via a biotinylated C terminus. The protein is subjected to a stretching force perpendicular to the glass when the magnet approaches the bead[9a] (Figure 1 A). The typical mechanical response of a protein L octamer to a changing force is shown in Figure 1 B. An applied force of 45 pN yields eight unfolding steps of approximately 15 nm. Quenching the force to 6.8 pN gives rise to two distinguishable contraction events.[7a, 11] First, an elastic contraction (EC) occurs immediately upon the change in force, driven by entropic collapse of the extended polypeptide that behaves as a pure polymer. Subsequently, a folding contraction (FC) as eight step-wise folding shortenings results from the sequential folding of each domain (ca. 9 nm; Figure 1 B).

Elastic and folding contractions do not change over long periods of time as long as the protein is allowed to refold completely, and kept mostly in the folded state. The trace shown in Figure 1 C illustrates this approach. A protein L octamer was probed cyclically with unfolding pulses to 54 pN followed by folding pulses to 6.6 pN. The cumulative time spent in the unfolded state can be controlled by changing the duty cycle of these folding/unfolding pulses. By contrast, after unfolding completely, a protein can be kept continuously in the unfolded state (Figure 1 D). Here, protein L is first unfolded at 45 pN, after which force is reduced to 14 pN. This force is sufficiently high as to prevent refolding events,

[*] Dr. J. Valle-Orero,[+] Dr. J. A. Rivas-Pardo,[+] Dr. R. Tapia-Rojo,
Dr. I. Popa, D. J. Echelman, Dr. S. Haldar, Prof. J. M. Fernández
Department of Biological Sciences, Columbia University
New York, NY 10027 (USA)
E-mail: jv2499@columbia.edu
jfernandez@columbia.edu

Dr. I. Popa
Current address: Department of Physics, University of Wisconsin
Milwaukee, WI 53211 (USA)

[+] These authors contributed equally to this work.

Supporting information and the ORCID identification number(s) for the author(s) of this article can be found under:
https://doi.org/10.1002/anie.201703630.
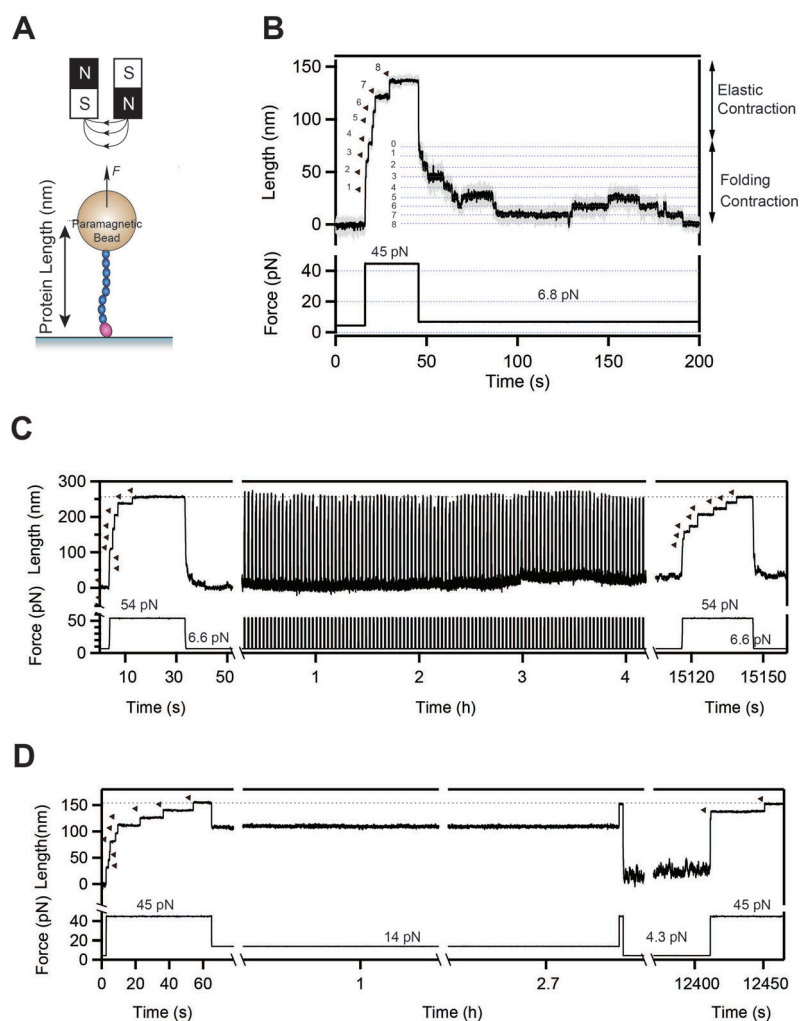
Figure 1. A) Scheme of the magnetic-tweezers setup with a tandem modular protein anchored to a glass surface and a paramagnetic bead. B) MT trace of a protein L octamer. The protein is first completely unfolded at 45 pN (8 unfolding steps marked by arrow heads), and then refolded at 6.8 pN. Refolding occurs in two phases: an elastic contraction followed by stepwise folding contractions (dashed lines mark each folding level). We use two kinds of force regimens to study protein ageing. The regimen shown in (C) keeps the protein mostly in the folded state, interrupted by brief unfolding pulses to probe the integrity of the protein. The regimen in (D) first fully unfolds and extends the protein, after which the force is lowered and the protein is kept unfolded at 14 pN. Afterwards, the protein is allowed to fold again at low force, followed by an unfolding pulse to check the number of domains still present (marked with arrows). A dashed line indicates total protein extension.

but low enough to reduce the rate of detachment of the biotin–streptavidin bond. After 4 hours in the unfolded state, only two domains are able to fold in the refolding pulse (4.3 pN), since they are observed in the second unfolding pulse.

Such long-term studies with magnetic tweezers are generally applicable to any protein. We have studied four proteins using this force-pulse regimen: protein L octamer, titin I10 and I91 octamers, and a nonamer of ubiquitin. Long-term unfolded exposure of each of these proteins causes a gradual loss in folding contraction, while the elastic recoil remains unchanged. Figure 2 A and Figure S2 A in the Supporting Information demonstrate these observations. An

initial unfolding pulse shows the normal response of a naïve protein. The protein is then kept unfolded for extended periods of time (Δt_u); subsequent force pulses reveal the loss of the folding contraction. This loss is observed in all proteins, despite their varied sequences and folds, however, the rates of loss differ considerably. We measured this rate in each protein by tracking the number of domains that unfold during periodic probe pulses to high forces after a refolding quench (Figure 2 C). The time course of domain loss while the protein is unfolded is a function of the time that cryptic side chains remain exposed to the solution. The rate of domain loss can be fitted with a single exponential (Figure 2 C), giving decay rates τ of 0.07 ± 0.02 h (I91), 0.09 ± 0.02 h (I10), 0.12 ± 0.03 h (ubiquitin), and 5.3 ± 1.4 h (protein L). Since protein L has the slowest decay, we chose this protein as a focus for subsequent studies under four different experimental conditions (Figure 2 D). The decay rate is slowed when the unfolding exposure is done in the dark, thus excluding photooxidation or photobleaching effects ($\tau = 12.6$ h ± 2.2). Similar experiments done in the presence of 5 mM ascorbic acid (AA), an antioxidant, greatly slowed the observed decay ($\tau = 66.8$ h ± 22.9). Figure 2 B shows a trajectory for protein L when AA was added to the solution. After 13 hours of continued exposure to the solvent, only a single domain is lost, thus demonstrating the powerful protective effect of antioxidants in slowing down protein ageing. We also tested the effects of the oxygen scavenger pyranose oxidase and catalase (POC),[12] and we observed a weaker effect than with AA ($\tau = 16.7$ h ± 2.8; Figure S3). Explicitly adding an oxidant (0.6 % hydrogen peroxide) accelerates domain loss ($\tau = 1.96$ h ± 0.4). By contrast, if the protein L octamer is kept mostly in the folded state, with only brief periodic unfolding pulses, the folding behavior of the protein remains unchanged for long periods of time ($\tau > 2220$ h ± 343; Figure S1).

The protection from domain loss by an antioxidant, and the acceleration of domain loss by a strong oxidant, suggests an underlying oxidative modification of side chains. Meanwhile, the long-term stability of protein L while folded (measured over a period of days) suggests that only cryptic side chains contribute to the accelerated ageing phenomenon. This accelerated ageing depends only on the cumulative unfolded time, and thus the cryptic-side-chain exposure time, independent of the experimental regimen (Figure S4). This phenomenon is irreversible, and occurs in an all-or-none manner; oxidized domains disappear one by one and are not recovered after long refolding pulses (Figures S2 and S5).
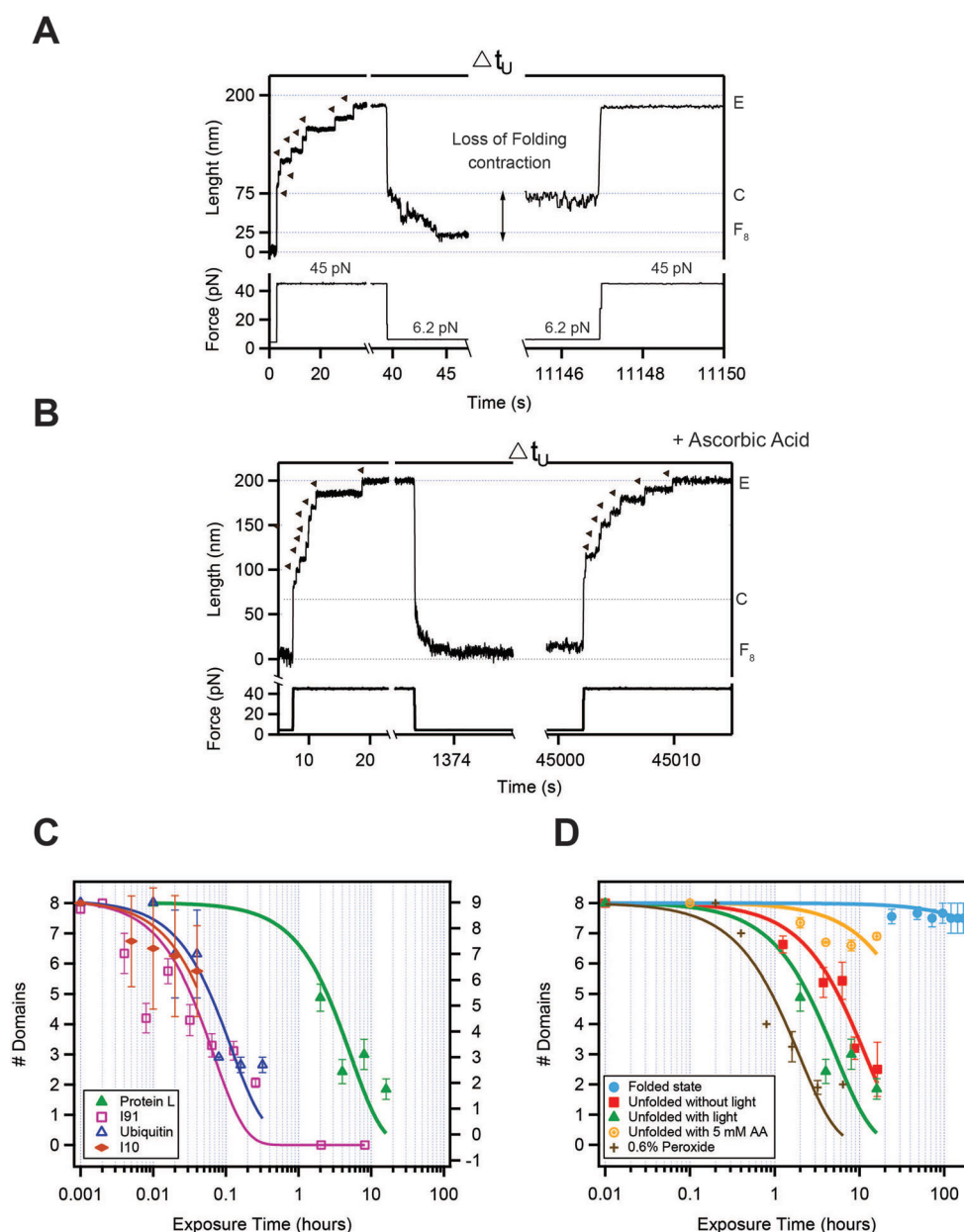
Figure 2. Time-dependent loss of folding contraction. A) Protein L octamer held in the extended state for $\Delta t_U > 3$ hrs shows a complete loss of its folding contraction, retaining only its elastic recoil. E = extended, C = collapsed, F_8 = fully folded. B) Protein L octamer is unfolded and held extended in a solution with 5 mm AA. After holding the protein unfolded for more than 12 hours, 7 of 8 domains are recovered. Arrows indicate unfolding steps. C) Number of folded domains that remain versus the time that a protein is exposed unfolded to the solvent Δt_U. The data are fitted with a single exponential (solid line), from which the decay rate τ and the standard error of the mean (SEM) are obtained. Four proteins were studied: I91 ($\tau = 0.07 \pm 0.02$ h; pink), I10 ($\tau = 0.09 \pm 0.02$ h; dark orange), ubiquitin (right y-axis; $\tau = 0.12 \pm 0.03$ h, dark blue) and protein L ($\tau = 5.3 \pm 1.4$ h, green). D) Protein L was studied under four conditions: 0.6% hydrogen peroxide added to the solution ($\tau = 1.96 \pm 0.4$ h; brown), 5 mm AA ($\tau = 66.8 \pm 22.9$ h; yellow), kept in the folded state at 4.3 pN ($\tau = 92.5 \pm 14.3$ days; blue), and without illumination ($\tau = 12.6 \pm 2.2$ h; red).

These findings allow us to quantify the elastic response of a protein after a mechanical deformation is removed. This expression provides a useful tool to predict how these mechanical properties are altered upon ageing, and ultimately how they compromise the integrity of tissues. The total recoil TR of an elastic protein can be written as [Eq. (1)]:

$$TR(F_{un}, F) = EC(F_{un}, F) + FC(F) \tag{1}$$

where the protein is released from an unfolding force F_{un} to a lower force F (Figure 3 A). The amplitude of the folding contraction is determined as the combination of the folding step size $ss(F)$ with the probability of folding $Pf(F)$, and the number N of domains ($FC(F) = N \cdot Pf(F) \cdot ss(F)$). The elastic contraction is simply the polymer collapse between F_{un} and F. All the components in Equation (1) can be readily determined experimentally from traces such as those in Figure 3 A. In these experiments, protein L octamers are first fully
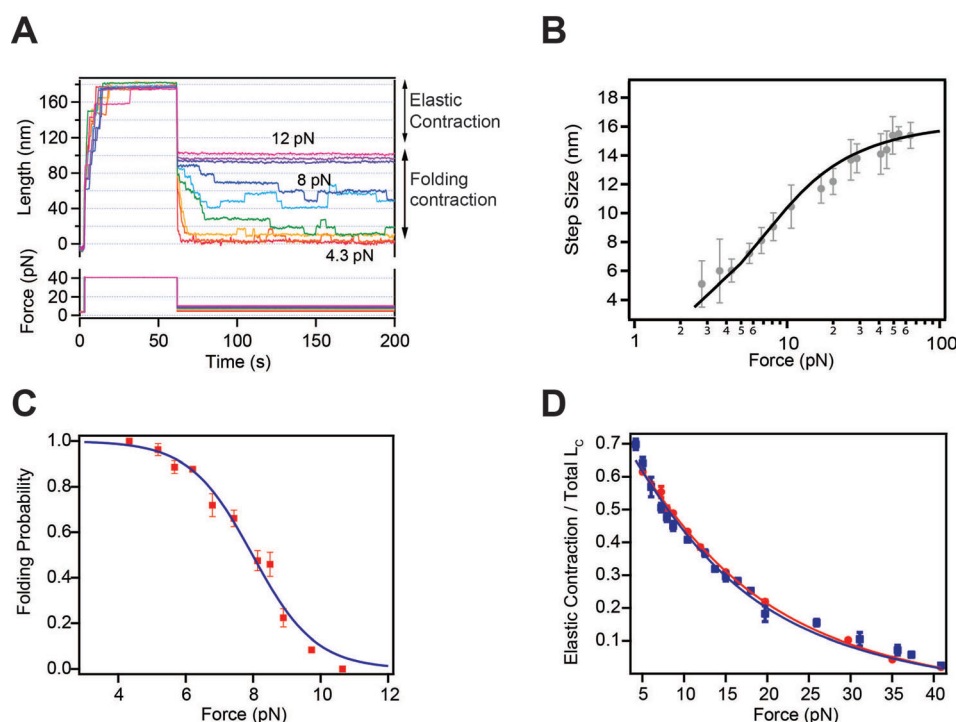
Figure 3. Dissecting protein folding under force into its components. A) A force quench results in a characteristic elastic contraction, followed by a force-dependent stepwise folding contraction. B) The average size of unfolding and folding steps as a function of force. The data are fitted using the FJC model with $l_k = 1.1$ nm and $\Delta L_c = 16.3$ nm. C) Folding probability as a function of refolding force. Data are fitted using a sigmoidal function with $m = 8$ pN and $r = 0.93$ pN. D) Elastic contraction measured from 45 pN to a refolding force F (40 to 4 pN) for a naïve protein (blue) and a fully oxidized protein (red). The fits correspond to the elastic recoil force dependency, assuming the FJC model with $l_k = 0.47$ nm, and normalized by the total contour length of each molecule. Error bars show the SEM.

unfolded at a high force of 45 pN, followed by a quench to 12–4.3 pN. The folding contraction begins at approximately 10 pN and is complete below around 5 pN. A salient feature of the folding contraction is the varying amplitude of the folding steps, which scales following the freely jointed chain (FJC) model of polymer elasticity (Figure 3 B). We fitted the data in Figure 3 B with the FJC equation defined as $ss(F) = \Delta L_c \mathcal{L}(F l_k/kT)$, where $\Delta L_c = 16.3$ nm is the contour length increment of a single protein L, $\mathcal{L}$ is the Langevin function, with F being the applied force, the Kuhn length $l_k = 1.1$ nm, and $kT = 4.1$ pN nm. From the same recordings we measure the folding probability, which is well described by a simple sigmoid as: $P_f(F) = 1 - 1/(1 + exp(-(F - m)/r))$ where $m = 8$ pN and $r = 0.93$ pN (Figure 3 C; see the Supporting Information). The elastic contraction is present in both the naïve and the fully aged protein as seen in Figure 2 A, and can be described by the FJC model. Figure 3 D shows the collapse from 45 pN to a lower force F. Remarkably, all data can be fitted with same Kuhn length $l_k = 0.47$ nm, thus showing that the modification of cryptic side chains does not alter the stiffness of the extended polypeptide chain.

Equation (1) readily predicts the total recoil observed in protein L octamers released from a high force F_{un} to a lower force F (Figure 4 A, red line). Figure 4 A illustrates the large contribution made by protein folding to the contractility of the protein L octamer, which reaches 50 % at $F \approx 6$ pN. It is clear from these data that the loss of the ability to fold severely compromises the mechanical integrity of the protein,

turning it into a much stiffer molecule. The time-dependent loss of folding contraction can now be incorporated into Equation (1) by multiplying by $\text{Ageing}(t) = e^{-\frac{t}{\tau}}$, where τ is the decay constant measured in Figure 2 C [Eq. (2)].

$$TR(F_{un}, F, t) = EC_{F_{un}-F} + FC(F) \cdot \text{Ageing}(t) \qquad (2)$$

Equation (2) is generally applicable to any elastic protein by simply adjusting the parameters described in Figure 3 to each protein, and the rate of domain loss measured in Figure 2. For example, in Figure 4 B we apply Equation (2) to proteins of the extracellular matrix (ECM), which are vital for maintaining tissue integrity. The elastic region of fibronectin is composed of 15 tandem repeats of FNIII-type domains, which unfold and refold in vivo in response to mechanical deformations.[13] By updating Equation (2) with the pertinent values[14] (Table S2), we can estimate the elastic recovery of young and aged fibronectin molecules deforming from a high force (20 pN in Figure 4 B) to a lower force F. Ageing causes a gradual reduction in the total recoil until the protein behaves as a mere polymer, where the loss of folding reduces its contractility up to 50 %. Ageing factors for elastic proteins in intact tissues have never been measured due to the complexity of the system and the large number of factors involved. To illustrate this scenario, we chose $\tau = 0.1$ h and $\tau = 70$ h, the time constants for the fastest and slowest decaying proteins observed in our measurements (Figure 2 C). We predicted the changes in the total recoil of this protein as

↖↖ These are not the final page numbers!

A

B
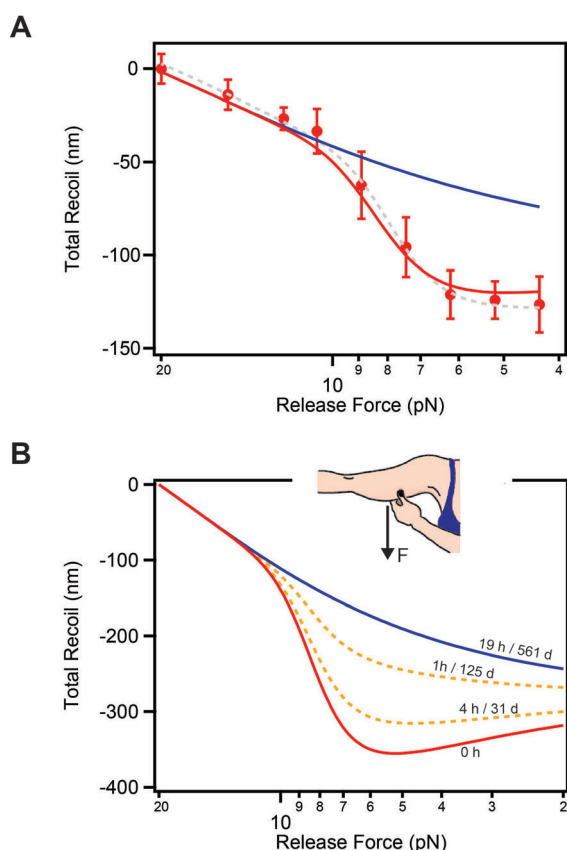
Figure 4. A) Total recoil (TR) of protein L from 20 pɴ to different release forces (15–4 pɴ). The experimental data (red symbols) are well reproduced by Equation (1) (red line) using the parameters of Figure 3. The elastic recoil is calculated for comparison (blue line). B) Model of the TR of 15 tandem FNIII domains, when the force is quenched from 20 pɴ to a lower force *F*. The change in TR is calculated with Equation (1) for an undamaged protein with its folding contraction intact (red line), compared to that of a damaged protein where the folding contraction is lost (blue line). Predictions of the change in TR for different accumulated ageing times at 6 pɴ are shown (dashed lines), using two ageing time constants $\tau = 0.1$ h and 70 h. The inset is an analogy of pinching the skin, which would apply a stretching force.

a function of the accumulated time spent in the unfolded state (Figure 4B). Taking the spontaneous unfolding and refolding rates of fibronectin (Table S2), we can estimate the fraction of time that the protein spends in the unfolded state at a physiological force of 6 pɴ. Total loss of the folding contraction is predicted to occur within 19 hours at the fastest decay rate, and 13,464 hours at the slowest decay rate that we measured. Other factors such as the concentration of reactive oxygen species (ROS) in the tissue and the presence of chaperones will likely affect the time course of ageing, however, these remain unknown.

A analogy for the cosmetic significance of protein ageing is shown in the inset in Figure 4B. An external perturbation (like a pinch of the skin) can expose the tissue to forces that will be transmitted to the ECM proteins in the connective tissue. If the proteins are unaffected by ROS, they will retract fully upon cessation of the perturbation, restoring the original

shape. By contrast, damaged proteins will retract less owing to their reduced contractility.

Our long-time-scale experiments reveal the cumulative effects of oxidative damage, which otherwise would manifest only after decades-long exposure. We propose that repeated mechanical deformation of tissues accelerates tissue ageing. Owing to the mechanical activity of the body, skin is exposed to repeated mechanical deformations throughout its lifetime. Skin deformation takes place under conditions of varying amounts of oxidative stress caused by exposure to UV light. As shown here, these conditions can cause accelerated protein ageing with its concomitant loss of mechanical integrity. Repeated exposure to mechanical shocks for brain tissue, as occurs in boxing and American football, may similarly trigger accelerated protein ageing of the elastic proteins that hold brain tissues together.[15]

All four proteins studied here undergo accelerated ageing when exposed to mechanical deformation, albeit at rates spanning from minutes to days. Damaged proteins lose their function and are forced into an irreversible and highly labile random coil. Such proteins are more susceptible to aggregation and protease digestion. The most obvious ways to slow ageing are to reduce the overall time a protein spends in the unfolded state and reduce the concentration of ROS present in the bathing solution. In this work, we have demonstrated methods that permit, for the first time, study of the slow irreversible effects of oxidative damage and ageing on elastic proteins, at time scales that are sufficiently long to be predictive for living organisms.

Conflict of interest

The authors declare no conflict of interest.

[1] B. Yu, S. Y. Kang, A. Akthakul, N. Ramadurai, M. Pilkenton, A. Patel, A. Nashat, D. G. Anderson, F. H. Sakamoto, B. A. Gilchrest, R. R. Anderson, R. Langer, *Nat. Mater.* **2016**, *15*, 911–918.

[2] M. J. Sherratt, *Adv. Wound Care* **2013**, *2*, 11–17.

[3] a) E. R. Stadtman, *Free Radical Res.* **2006**, *40*, 1250–1258; b) A. M. de Graff, M. J. Hazoglou, K. A. Dill, *Structure* **2016**, *24*, 329–336; c) A. R. Hipkiss, *Exp. Gerontol.* **2006**, *41*, 464–473; d) T. Finkel, N. J. Holbrook, *Nature* **2000**, *408*, 239–247.

[4] a) T. Nyström, *EMBO J.* **2005**, *24*, 1311–1317; b) E. R. Stadtman, *Science* **1992**, *257*, 1220–1224; c) L. Gorisse, C. Pietrement, V. Vuiblet, C. E. Schmelzer, M. Kohler, L. Duca, L. Debelle, P. Fornes, S. Jaisson, P. Gillery, *Proc. Natl. Acad. Sci. USA* **2016**,

113, 1191–1196; d) R. S. Rao, I. M. Moller, *Proteomics* **2011**, *11*, 4166–4173.

[5] a) B. S. Berlett, E. R. Stadtman, *J. Biol. Chem.* **1997**, *272*, 20313–20316; b) B. Halliwell, J. M. C. Gutteridge, *Free radicals in biology and medicine*, 5th ed., Oxford University Press, Oxford, **2015**.

[6] a) K. Akhtar, T. J. Broekelmann, M. Miao, F. W. Keeley, B. C. Starcher, R. A. Pierce, R. P. Mecham, T. L. Adair-Kirk, *J. Biol. Chem.* **2010**, *285*, 37396–37404; b) G. Degendorfer, C. Y. Chuang, H. Kawasaki, A. Hammer, E. Malle, F. Yamakura, M. J. Davies, *Free Radical Biol. Med.* **2016**, *97*, 602–615.

[7] a) J. M. Fernandez, H. Li, *Science* **2004**, *303*, 1674–1678; b) J. Valle-Orero, E. C. Eckels, G. Stirnemann, I. Popa, R. Berkovich, J. M. Fernandez, *Biochem. Biophys. Res. Commun.* **2015**, *460*, 434–438.

[8] a) J. Alegre-Cebollada, P. Kosuri, D. Giganti, E. Eckels, J. A. Rivas-Pardo, N. Hamdani, C. M. Warren, R. J. Solaro, W. A. Linke, J. M. Fernandez, *Cell* **2014**, *156*, 1235–1246; b) A. E. Beedle, S. Lynham, S. Garcia-Manyes, *Nat. Commun.* **2016**, *7*, 12490.

[9] a) I. Popa, J. A. Rivas-Pardo, E. C. Eckels, D. J. Echelman, C. L. Badilla, J. Valle-Orero, J. M. Fernandez, *J. Am. Chem. Soc.* **2016**, *138*, 10546–10553; b) J. Valle-Orero, J. A. Rivas-Pardo, I. Popa, *Nanotechnology* **2017**, *28*, 174003.

[10] I. Popa, R. Berkovich, J. Alegre-Cebollada, C. L. Badilla, J. A. Rivas-Pardo, Y. Taniguchi, M. Kawakami, J. M. Fernandez, *J. Am. Chem. Soc.* **2013**, *135*, 12762–12771.

[11] J. A. Rivas-Pardo, E. C. Eckels, I. Popa, P. Kosuri, W. A. Linke, J. M. Fernandez, *Cell Rep.* **2016**, *14*, 1339–1347.

[12] M. Swoboda, J. Henig, H. M. Cheng, D. Brugger, D. Haltrich, N. Plumere, M. Schlierf, *ACS Nano* **2012**, *6*, 6364–6369.

[13] a) L. Li, H. H. Huang, C. L. Badilla, J. M. Fernandez, *J. Mol. Biol.* **2005**, *345*, 817–826; b) G. Baneyx, L. Baugh, V. Vogel, *Proc. Natl. Acad. Sci. USA* **2002**, *99*, 5139–5143.

[14] a) M. J. Bradshaw, M. L. Smith, *Biophys. J.* **2011**, *101*, 1740–1748; b) A. F. Oberhauser, C. Badilla-Fernandez, M. Carrion-Vazquez, J. M. Fernandez, *J. Mol. Biol.* **2002**, *319*, 433–447.

[15] a) A. C. McKee, R. C. Cantu, C. J. Nowinski, E. T. Hedley-Whyte, B. E. Gavett, A. E. Budson, V. E. Santini, H. S. Lee, C. A. Kubilus, R. A. Stern, *J. Neuropathol. Exp. Neurol.* **2009**, *68*, 709–735; b) M. T. K. Kirkcaldie, J. M. Collins, *J. Chem. Neuroanat.* **2016**, *76*, 9–18; c) B. Lichtenberg, E. M. Mandelkow, T. Hagestedt, E. Mandelkow, *Nature* **1988**, *334*, 359–362.
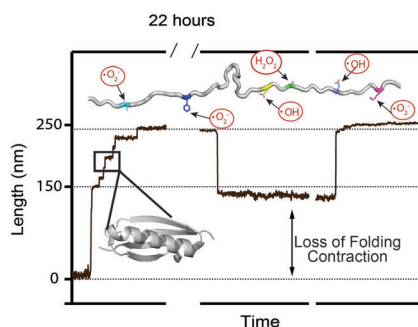
↖↖ These are not the final page numbers!

Communications

Proteins

J. Valle-Orero,* J. A. Rivas-Pardo,
R. Tapia-Rojo, I. Popa, D. J. Echelman,
S. Haldar,
J. M. Fernández* —————— ▪▪▪▪–▪▪▪▪

Mechanical Deformation Accelerates
Protein Ageing

Time will tell: Accelerated ageing occurs when a protein is held unfolded under force for long periods of time. Maintaining a protein extended for more 20 h blocks its ability to refold. This loss of folding contraction is triggered by the exposure of cryptic side chains to the oxidative environment, and can be greatly slowed by antioxidants. This kind of oxidative damage is a hallmark of the loss of tissue elasticity that occurs during ageing.

© 2017 Wiley-VCH Verlag GmbH & Co. KGaA, Weinheim

These are not the final page numbers! ↗↗